An Analytical Approach to Synthesis and Modeling of Torque Control Strategy for Two-Mass Resonant Systems

Ghazanfar Shahgholian[1], Jawad Faiz[2]

Abstract –*Torsional oscillations due to rotor dynamic are very important in power system dynamic analysis. The major problem in torsional oscillation in flexible system is the result of connecting a load to motor with long axis. A simple model of this sample mechanical resonant system is a two-mass system such as industrial motor drives. In this paper PID, PID_P and modify PID controllers is applied in order to control torque of a two-mass system. The pole-placement controller such as coefficient diagram method (CDM) and integral of time multiplied by absolute error (ITAE) is used to assign closed-loop poles of the system characteristic equation. A complete state-space mathematical model for two-mass resonant system is first developed and behavior dynamic appointment roots locus of characteristic equation is analyzed The dynamic analysis is verified by transfer function simulation using Matlab and time domain simulation of the two-mass system. Finally, advantages of the proposed design method are demonstrated in the cases of torque control and corr-esponding results are compared.*

Keywords: *two-mass system, simulation and design, PID controller, coefficient diagram method.*

I. Introduction

With the progress of robust control techniques, high performance in the motion control field has been realized. In general motion control applications, the plant consists of a motor, a geared transmission, and load. In some industrial applications such as rolling mill drives, long shaft driving systems, and industrial robots, mechanical part of the system has very low resonant frequency; the reason is a long shaft between the motor and its load. Mechanical resonance is one of the most common problems that designers face when trying to maximize either command response or dynamic stiffnes-s. Any simplified model has equivalent inertia, damping and stiffness characteristics. In many cases, it is roughly modeled by a two-mass system in which only the first resonant mode is considered [1, 2].

Vibration is an impediment to enhance the performa-nce of the system. Many methods have been so far pres-ented for the control of two-mass system such as resonance ratio control [3], H_∞ control [4, 5], pole placement method [6], I-P controller [7] and optimal control [8]. A motion control strategy for high speed industrial robots with high accuracy has been proposed in [9], where for resonant vibration, reference filtering method consists of a notch filter and a phase compensat-ion gain is used. In [10], a discrete-time sliding mode control has been applied to a two-mass system coupled to a flexible shaft where a full order observer is used to estimate the necessary state variables. A systematic co-mparative study of compensation schemes such as reso-nance ratio control and proportional integral derivative (PID) control for the coordinated motion control of two-inertia mechanical systems presented in [11]. In [12], an additional feedback from the derivate of the shaft torque applied to both two- and three-mass systems in order to estimate torsional torque. A novel identification method based on a modified plant (instead of a original plant) is proposed in [13], when one of the output variables is considered as control feedback.

In the design of a linear time-invariant control system using classical control theory, the first step is to choose the controller type. In most cases, the cost of control sy-stem increases with its complexity. PID controllers are the widely used one in industrial processes, because of the good performance over a large range of operation conditions and their functional simplic ty [14]. PID con-trol with its three terms functionality covering treatment to both transient and steady-states response, offers the simplest and yet most efficient solution for many real control problems. One of the most widely used control laws in two-mass systems is the PID type controller. In the torque control of two-mass resonant system, in order to suppress the mechanical resonance, PID control was often used as a simple control method. Consequently, for high-bandwidth motion control applications, PID controllers cannot impart the desired levels of dynamic performance in the presence of extraneous inputs.

The first step in the analysis and design of control systems is mathematical modeling of the system. The two most common control methods are transfer function approach and state equation approach. The main aim of this paper is the application of a PID controller to torque control of a two-mass resonant system. An analytical approach for modeling of two-mass system is proposed, and an optimal controller is introduced by pole placeme-nt controller using three different criteria in order to tra-nsfer the torque well.

Manuscript received and revised June 2009, accepted July 2009

The article is organized as follows: following the introduction, identification of a complete state-space mathematical model of a two-mass resonant system for multi-input single-output is developed in section II. Design of a PID controller based on transfer function of the plant model is described in section III. In section IV eigenvalue technique is used to investigate the effect of the PID controller on the oscillations and system stability. Proposed controller structure and problem formulation are described in Section V. Simulation results are presented and discussed in section VI and conclusions are given in section VII.

II. Study System and Mathematical Model

Torsional vibration involves transfer of power between two or more connected rotating masses. A m-order rotational mass mechanical system has (m-1) torsional modes whose frequencies are natural frequencies of the mechanical system oscillation. The torsional relation of the I^{th} mass spring system has been shown in Fig. 1. The torque equilibrium of the I^{th} mass spring system has the following linear form:

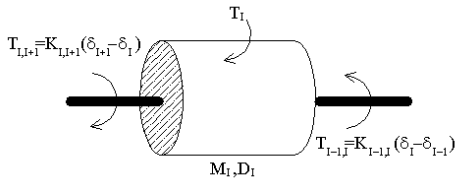

Fig. 1: I^{th} mass spring system

$$J_I \frac{d}{dt}(\Delta\omega_I) = T_I + K_{I,I+1}(\delta_{I+1} - \delta_I) - K_{I-1,I}(\delta_I - \delta_{I-1}) - B_I(\Delta\omega_I) \quad (1)$$

where for a I^{th} mass, J_I is the inertia constant, B_I is the damping coefficient and K_I is the stiffness shaft. Also, there is no torsional torque at the two extremes of the shaft. Therefore, for I=1, 2, …, m we have:

$$\begin{cases} K_{I-1,I}\big|_{I=1} = 0 \\ K_{I,I+1}\big|_{I=m} = 0 \end{cases} \quad (2)$$

The simplest model of such resonant mechanical system is two-mass system. The general configuration of a two-mass resonant system which has a motor and a load connected to a flexible shaft has been shown in Fig. 2. The system parameters used in this paper are listed on Table I.

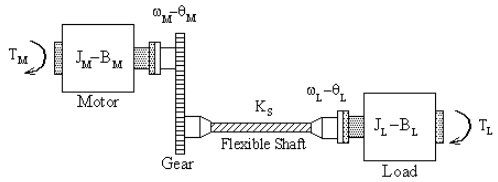

Fig. 2: Plant model of a two-mass resonant system

TABLE I
NOMINAL PARAMETERS OF A TWO-MASS PLANT

Component	Quantity	Rating value
K_S	shaft stiffness	138 Nm/rad
B_S	shaft damping coefficient	1×10^{-1} Nm/rad/s
J_M	motor inertia	4.8×10^{-2} kg.m^2
B_M	motor viscosity coefficient	1.3×10^{-3} Nm/rad/s
J_L	load inertia	8.6×10^{-3} kg.m^2
B_L	load viscosity coefficient	6.9×10^{-2} Nm/rad/s

A simple state-space model of a two-mass system with the following state variables: motor angular velocity (ω_M), load angular velocity (ω_L), angle of motor (θ_M), angle of load (θ_L), two inputs of motor torque (T_M) and load disturbance torque (T_L) is given as follows:

$$\dot{\omega}_M = \frac{B_S}{J_M}\omega_L - \frac{B_M + B_S}{J_M}\omega_M - \frac{K_S}{J_M}(\theta_M - \theta_L) + \frac{1}{J_M}T_M \quad (3)$$

$$\dot{\omega}_L = \frac{B_S}{J_L}\omega_M - \frac{B_S + B_M}{J_L}\omega_L + \frac{K_S}{J_L}(\theta_M - \theta_L) - \frac{1}{J_L}T_L \quad (4)$$

$$\dot{\theta}_M = \omega_M \quad (5)$$

$$\dot{\theta}_L = \omega_L \quad (6)$$

where J_M is the motor inertia, J_L is the load inertia, B_M is the motor viscous damping coefficient, and B_L is the load viscous damping coefficient. Equivalent spring constant of the shaft, K_S, provides a load proportional to the difference of motor and load positions. Also, to represent loss producing properties, a mechanical damping term is shown developing torque proportional to velocity differences via cross-coupled viscous damping, B_S. The shaft torsional torque (T_S) is given by:

$$T_S(s) = B_S[\omega_M(s) - \omega_L(s)] + K_S[\theta_M(s) - \theta_L(s)] \quad (7)$$

Block diagram of the compliantly coupled mechanism has been shown in Fig. 3. Transfer functions of the motor, load and shaft are $G_M(s)=1/(J_Ms+B_M)$, $G_L(s)=1/(J_Ls+B_L)$ and $G_S(s)=B_S+K_S/s$, respectively.

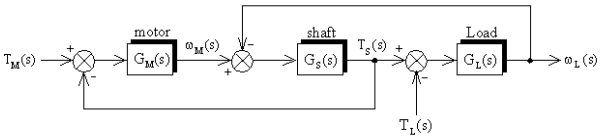

Fig. 3: Block diagrm of a two-mass mechanical system

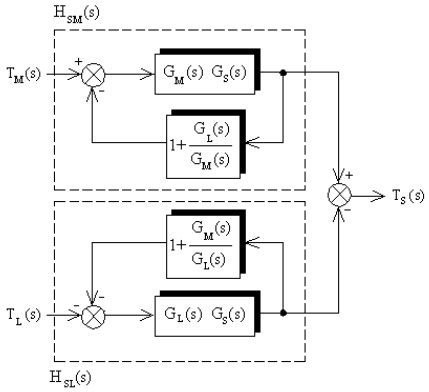

Fig. 4: Block diagrm of a two-mass resonant system

Let a two-input single-output process be represented by the block diagram shown in Fig. 4. The shaft torque is as follows:

$$T_S(s)=\underbrace{\frac{G_M(s)G_S(s)}{1+G_M(s)G_S(s)+G_L(s)G_S(s)}}_{H_{SM}(s)}T_M(s)+\underbrace{\frac{G_L(s)G_S(s)}{1+G_M(s)G_S(s)+G_L(s)G_S(s)}}_{H_{SL}(s)}T_L(s) \tag{8}$$

where open-loop transfer function is given by (6), from shaft to load torque, and by (7) from shaft to motor torque.

$$H_{SL}(s)=\left.\frac{T_S(s)}{T_L(s)}\right|_{T_M=0}=\frac{1}{J_L J_M}\frac{(B_S s+K_S)(J_M s+B_M)}{\Delta(s)} \tag{9}$$

$$H_{SM}(s)=\left.\frac{T_S(s)}{T_M(s)}\right|_{T_L=0}=\frac{1}{J_L J_M}\frac{(B_S s+K_S)(J_L s+B_L)}{\Delta(s)} \tag{10}$$

where the characteristic equation of the open-loop system is given as follows:

$$\Delta(s)=s^3+\left(\frac{B_M+B_S}{J_M}+\frac{B_L+B_S}{J_L}\right)s^2+\left(\frac{K_S(J_M+J_L)+B_S(B_M+B_L)+B_M B_L}{J_M J_L}\right)s+\frac{K_S(B_M+B_L)}{J_M J_L} \tag{11}$$

There are three poles for the characteristic equation, one real pole p_1 is negative and a pair of complex conjugate poles $p_{2,3}$ are in the left half plane and close to the imaginary axis. The root locus diagram of open-loop system to the variation of the K_S has been shown in Fig. 5.

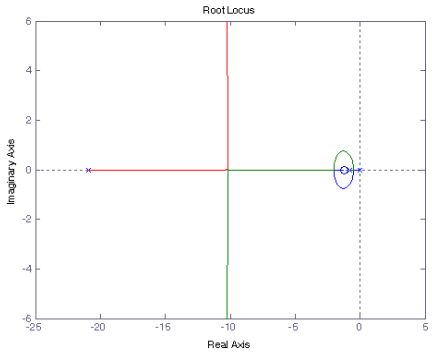

Fig. 5: Root locus diagrm of a open-loop system

Two-mass systems are the vibratory systems that have poles on/near the imaginary axis. Natural frequency (ω_R) and damping ratio (η) of the system are given by:

$$\begin{cases}\omega_R=\sqrt{\frac{K_S}{J_L}\left(1+\frac{J_L}{J_M}\right)}\\ \eta=\frac{B_S}{2}\sqrt{\frac{1}{K_S J_L}\left(1+\frac{J_L}{J_M}\right)}\end{cases} \tag{12}$$

An increase in the motor inertia constant decreases both ω_R and η. Conversely, increasing K_S coefficient increases ω_R and decrease η. An increase in B_S coefficient increases η without affecting ω_R. Also, (12) (this no is it correct?) indicates that large systems, which have large inertias, generally produce low natural frequencies. Smaller systems, which have relatively small inertias and stiff components, generally produce higher natural frequencies. The response frequency of transfer functions relative to motor torque and load disturbance torque have been shown in Figs. 6 and 7, respectively. In this figures, the dashed line, the thick solid line and the dashed–dotted line show the corresponding motor speed, load speed and shaft torque. One peak arises in the gain characteristic plot at frequency ω_R. The dominant eigenvalues for open-loop system are: P_1=-1.2426 and $p_{2,3}$=-10.26±j137.14. The resonant frequency is ω_R=137.6 rad/s and anti-resonant frequency is ω_A=126.7 rad/s. The damping factor of the original plant without the controller is η=0.0498. Since all eigenvalues of the system are on the left hand of the plane, the system is stable but highly damped. In the open-loop system with step response shown in Fig. 8, there are large oscillations between 0 to 0.3 seconds. Dynamic response of T_S to a step input T_M (solid line) and T_L (dash line), have been presented in Fig. 8 respectively.

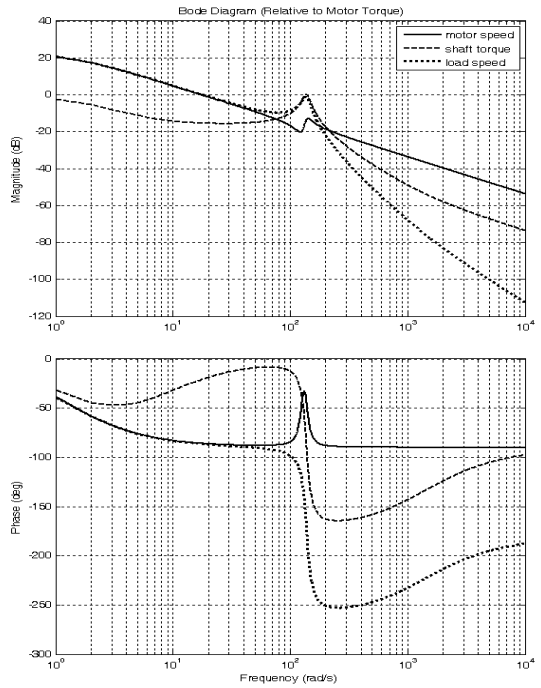

Fig. 6: Response frequency of transfer function relative to motor torque

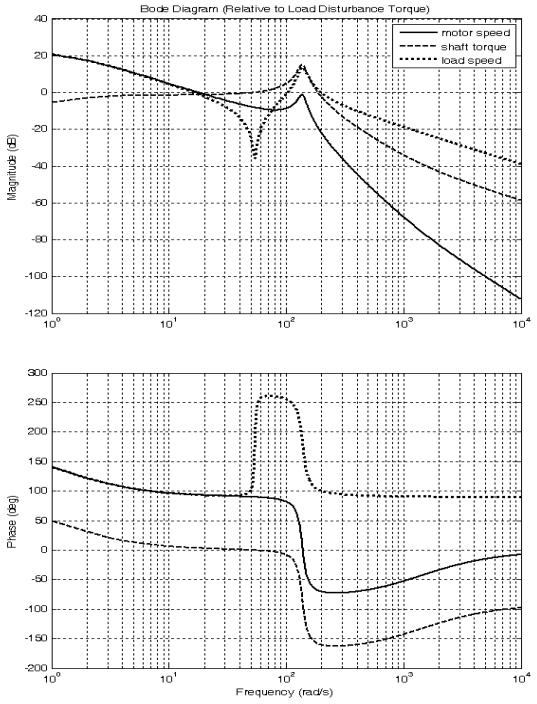

Fig. 7: Response frequency of transfer function relative to load disturbance torque

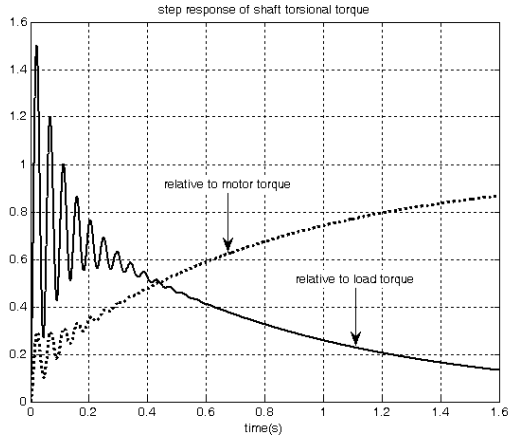

Fig. 8: Step response of shaft torque in open-loop system

III. PID Controller Design

Control systems are designed to perform specific tasks. Generally, tasks of control systems can be divided into two categories: stabilization or regulation and tracking or servo. A typical control system consists of four parts: a plant to be controlled, sensors for measurement, actuators for control action and a control law. Nowadays, despite of many proposed modern controller design methods, use of classical controller design methods is still popular. In a system controller design, all states of the system are not measurable. It is often impossible to measure ω_L, T_S and T_L in a real system. Large load inertia and thin shaft make vibration suppression of the torsional system more difficult. In the controller design, several objectives and constraints must be taken into consideration. The main objective is damping of the oscillations. However, the controller is not allowed to change the stationary torque. In order to suppress mechanical response a PID control (as a simple control method) is often used in the torque control of two mass resonant. Block diagram of the torque control system using PID controller, $G_T(s)$, has been shown in Fig. 9.

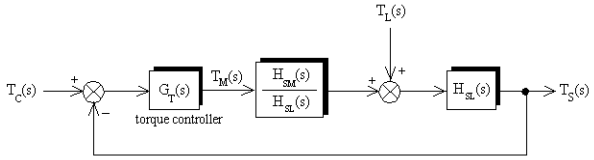

Fig. 9. Torque control system using PID controller

The controller have a proportional term K_P, an integration term K_I and a derivative term K_D. They can be described by the following transfer function:

$$G_T(s) = K_P + \frac{K_I}{s} + K_D\, s \tag{13}$$

Therefore, transfer function of the close-loop system between the shaft torsional output torque $T_S(s)$ and input torque command $T_C(s)$ is given by:

$$H_{TC}(s)=\left.\frac{T_S(s)}{T_C(s)}\right|_{T_L=0}=\frac{G_T(s)H_{SM}(s)}{1+G_T(s)H_{SM}(s)} \quad (14)$$

and transfer function between the output $T_S(s)$ and torque disturbance $T_L(s)$ is given by:

$$H_{TL}(s)=\left.\frac{T_S(s)}{T_L(s)}\right|_{T_C=0}=\frac{H_{SL}(s)}{1+G_T(s)H_{SM}(s)} \quad (15)$$

Shaft torque is as follows:

$$T_S(s)=H_{TC}(s)T_C(s)-H_{TL}(s)T_L(s) \quad (16)$$

Shaft torque transfer function $H_{TC}(s)$, which is most important in the close-loop design with PID controller, is given by:

$$H_{TC}(s)=\frac{N_{TC}(s)}{D_{TC}(s)}=K_T+\frac{\sum_{k=0}^{k=3}\beta_k s^k}{\sum_{k=0}^{k=4}\alpha_k s^k} \quad (17)$$

where $N_{TC}(s)$ and $D_{TC}(s)$ are respectively the numerator polynomial and the denominator of the close-loop transfer function:

$$\begin{aligned}N_{TC}(s)=&\underbrace{K_D J_L B_S}_{n_4}s^4+\underbrace{[K_D(J_L K_S+B_L B_S)+K_P J_L B_S]}_{n_3}s^3\\&+\underbrace{[K_I J_L B_S+K_P(K_S J_L+B_L B_S)+K_D K_S B_L]}_{n_2}s^2\\&+\underbrace{[K_P K_S B_L+K_I(K_S J_L+B_L B_S)]}_{n_1}s+\underbrace{K_I K_S B_L}_{n_o}\end{aligned} \quad (18)$$

$$\begin{aligned}D_{TC}(s)=&\underbrace{(J_M J_L+n_4)}_{d_4}s^4+\underbrace{[J_M B_L+B_M J_L+B_S(J_L+J_M)+n_3]}_{d_3}s^3\\&+\underbrace{[B_M B_L+B_S(B_L+B_M)+K_S(J_L+J_M)+n_2]}_{d_2}s^2\\&+\underbrace{[K_S(B_L+B_M)+n_1]}_{d_1}s+\underbrace{K_I K_S B_L}_{d_0}\end{aligned} \quad (19)$$

To simplify the analysis, numerator and denominator coefficients of the normalized system's closed-loop transfer function can be arranged as:

$$\begin{cases}\alpha_k=\dfrac{1}{d_4}(n_k-\dfrac{n_4}{d_4}d_k) & k=1,2,3\\ \beta_k=\dfrac{d_k}{d_4} & k=1,2,3,4\\ K_T=\dfrac{n_4}{d_4}\end{cases} \quad (20)$$

Characteristic equation $D_{TC}(s)$, denominator polynomial $H_{TC}(s)$, is 4th- order. The signal flow graph of the close system with a PID controller has been shown in Fig. 10. Dynamic equation of the close-loop two-mass system with four state variables (x_1, x_2, x_3, x_4), in controllable canonical form is as follows:

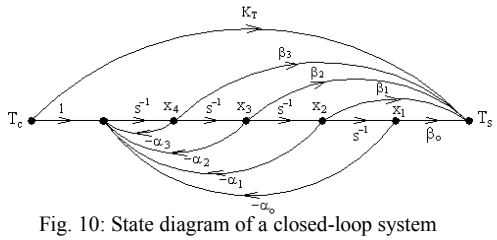

Fig. 10: State diagram of a closed-loop system

$$\frac{d}{dt}\begin{bmatrix}x_1\\x_2\\x_3\\x_4\end{bmatrix}=\begin{bmatrix}0&1&0&0\\0&0&1&0\\0&0&0&1\\-\alpha_0&-\alpha_1&-\alpha_2&-\alpha_3\end{bmatrix}\begin{bmatrix}x_1\\x_2\\x_3\\x_4\end{bmatrix}+\begin{bmatrix}0\\0\\0\\1\end{bmatrix}[T_C]$$

$$[T_S]=[\beta_0\quad\beta_1\quad\beta_2\quad\beta_3]\begin{bmatrix}x_1\\x_2\\x_3\\x_4\end{bmatrix}+[K_T][T_C] \quad (21)$$

The observer canonical form realization is as follows:

$$\frac{d}{dt}\begin{bmatrix}x_1\\x_2\\x_3\\x_4\end{bmatrix}=\begin{bmatrix}0&0&0&-\alpha_0\\1&0&0&-\alpha_1\\0&1&0&-\alpha_2\\0&0&1&-\alpha_3\end{bmatrix}\begin{bmatrix}x_1\\x_2\\x_3\\x_4\end{bmatrix}+\begin{bmatrix}\beta_0\\\beta_1\\\beta_2\\\beta_3\end{bmatrix}[T_C]$$

$$[T_S]=[0\quad 0\quad 0\quad 1]\begin{bmatrix}x_1\\x_2\\x_3\\x_4\end{bmatrix}+[K_T][T_C] \quad (22)$$

This state equation describes the system by combining the plant and the controller. Dynamic response of a linear system is governed by the magnitude and location of its eigenvalues, or poles. A PID controller based on the pole assignment method can improve the system characteristics such that the closed-loop system performance will satisfy the requirement criteria. Since damping losses usually considered being relatively low, they are neglected without significant affect on the accuracy of the forgoing analysis [15].

III.1. Coefficient diagram method

In coefficient diagram method (CDM), performance, stability index γ_k and equivalent time constant τ are specified in the closed-loop transfer function, related to the controller parameters algebraically in explicit form. The PID controllers' gains are designed by using the standard form of CDM as follows [16]:

$$\begin{cases} K_P = \dfrac{\omega_R^2}{2 K_J \omega_A^2}[(\dfrac{\omega_G}{\omega_R})^2 - 1] \\ K_I = \dfrac{\omega_R^3}{K_J \omega_A^2 \sqrt{8}\ \gamma_1 \sqrt{\gamma_2}}[(\dfrac{\omega_G}{\omega_R})^2 + 1]^{\frac{3}{2}} \\ K_D = \dfrac{\sqrt{\gamma_2}\ \omega_R}{\sqrt{2}\ K_J \omega_A^2}\sqrt{(\dfrac{\omega_G}{\omega_R})^2 + 1} \end{cases} \quad (23)$$

where ω_G and τ are the gain crossover frequency and equivalent time constant, respectively:

$$\begin{cases} \tau = \dfrac{\gamma_1 \sqrt{2\gamma_2}}{\sqrt{\omega_R^2 + \omega_G^2}} \\ \omega_G = \sqrt{\omega_R^2 + \dfrac{2 K_S K_{PT}}{J_M}} \end{cases} \quad (24)$$

III.2. Pole placement Control (PPC)

Pole location must be chosen carefully and wisely, and this needs deep insight to the system characteristics. The generic characteristic equation of a 3rd-order polynomial with two pairs of complex and one real root is [2]:

$$\begin{aligned} \Delta(s) &= (s+\alpha)(s^2 + 2\eta\omega_n s + \omega_n^2) \\ &= s^3 + \alpha(2\eta+1)s^2 + (\omega_n^2 + 2\eta\alpha\omega_n)s + \alpha\omega_n^2 \end{aligned} \quad (25)$$

Here, we make pole arrangement like (22) to design the parameters of the controller. Equating the coefficients of $D_{TC}(s)$ and $\Delta(s)$, and defining η=1, the following relationships are obtained:

$$\begin{cases} \dfrac{K_{DT} K_S}{J_M} = 3\alpha \\ \dfrac{K_{PT} K_S}{J_M} + \omega_R^2 = 2\alpha\omega_n + \omega_n^2 \\ \dfrac{K_{IT} K_S}{J_M} = \alpha\omega_n^2 \end{cases} \quad (26)$$

From (21), the value of α is given by:

$$\alpha = \frac{\omega_R^2}{4\omega_n}\left[(\frac{\omega_G}{\omega_R})^2 + 1 - 2(\frac{\omega_n}{\omega_R})^2\right] \quad (27)$$

III.3. ITAE Criterion

The gains controller is evaluated using the integral of time multiplied by the absolute error (ITAE) criterion for a step reference input. The ITAE performance index provides the best selectivity by minimizing overshoot and settling time for a given undershoot. As for the ITAE criterion, the standard form coefficients for a step input are given in Table II, where ω_n represents the 3dB bandwidth [4].

TABLE II
MINIMUM ITAE STANDARD FOR A STEP INPUT

Denominator
$s^3 + 1.75\omega_n s^2 + 2.15\omega_n^2 s + \omega_n^3$
$s^4 + 2.1\omega_n s^3 + 3.4\omega_n^2 s^2 + 2.7\omega_n^3 s + \omega_n^4$
$s^5 + 2.8\omega_n s^4 + 5.0\omega_n^2 s^3 + 5.5\omega_n^3 s^2 + 3.4\omega_n^4 s + \omega_n^5$

The coefficients that will minimize the ITAE performance criterion for a step input have been determined for a general closed-loop transfer function. The gains of the controller obtained from ITAE criterion are given by:

$$\begin{cases} K_D = \dfrac{1.75\omega_n J_M}{K_S} \\ K_P = \dfrac{2.15\omega_n^2 J_M - J_M \omega_R^2}{K_S} \\ K_I = \dfrac{J_M \omega_n^3}{K_S} \end{cases} \quad (28)$$

From (21), ω_n is given by:

$$\omega_n = \sqrt{\frac{\omega_G^2 + \omega_R^2}{4.3}} \quad (29)$$

IV. Feedback Compensation

A block diagram of the torque control system using PID controller, $G_T(s)$, with feedback compensation, $G_F(s)$, is shown in Fig. 11.

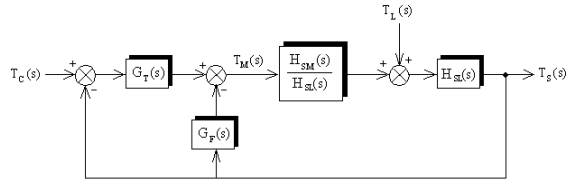

Fig. 11. Torque control system using PID controller with feedback compensation

The transfer function of the close-loop system between shaft the torsional torque output $T_S(s)$ and torque command input, $T_C(s)$, and the transfer function between the output $T_S(s)$ and torque disturbance $T_L(s)$ are given by:

$$H_{CF}(s)=\left.\frac{T_S(s)}{T_C(s)}\right|_{T_L=0}=\frac{G_T(s)H_{SM}(s)}{1+[G_T(s)+G_F(s)]H_{SM}(s)} \tag{30}$$

$$H_{LF}(s)=\left.\frac{T_S(s)}{T_L(s)}\right|_{T_C=0}=\frac{H_{SL}(s)}{1+[G_T(s)+G_F(s)]H_{SM}(s)} \tag{31}$$

From (11) and (25), I-PD, ID-P and PID-P controllers have the same characteristic equations and it can be seen that the zero are different. Therefore, the overshoot in the shaft torque, for a step change in the input reference, is expected to be smaller for the I-P control.

V. Modified PID Controller Structure

The proposed controller structure consists of an integral controller in the feed-forward path and also a PD controller in the feedback path. The modified PID controller (MPID) can be given as a integral controller, proportional derivative controller and a 1st-order time delay. A block diagram of the torque control system using MPID has been shown in Fig. 12, where $G_I(s)=K_I/s$, $G_P(s)=K_P+sK_D$ and $G_D(s)=1/(1+T_Ds)$.

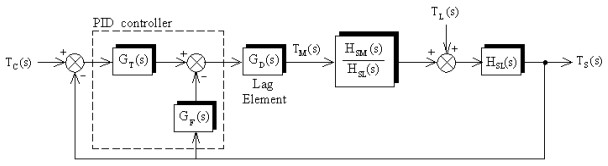

Fig. 12: Torque control system using modified PID controller

$$\frac{d}{dt}\omega_M=-\frac{B_M}{J_M}\omega_M-\frac{1}{J_M}T_S+\frac{1}{J_M}T_M \tag{32}$$

$$\frac{d}{dt}T_S=(K_S-\frac{B_MB_S}{J_M})\omega_M-(K_S-\frac{B_LB_S}{J_L})\omega_L$$
$$-B_S(\frac{1}{J_M}+\frac{1}{J_L})T_S+\frac{B_S}{J_M}T_M+\frac{B_S}{J_L}T_L \tag{33}$$

$$\frac{d}{dt}\omega_L=-\frac{B_L}{J_L}\omega_L+\frac{1}{J_L}T_S-\frac{1}{J_L}T_L \tag{34}$$

$$\frac{d}{dt}e_T=K_I(T_C-T_S) \tag{35}$$

$$\frac{\mathrm{d}}{\mathrm{dt}}\mathrm{T_M}=-\frac{1}{\mathrm{T_D}}\mathrm{T_M}+\frac{1}{\mathrm{T_D}}\mathrm{e_T}-\frac{\mathrm{K_P}}{\mathrm{T_D}}\mathrm{T_S}$$
$$-\frac{K_D}{T_D}(K_S-\frac{B_MB_S}{J_M})\omega_M+\frac{K_D}{T_D}(K_S-\frac{B_LB_S}{J_L})\omega_L \tag{36}$$

Characteristic equation of the close-loop system with MPID controller is given as follows:

$$\Delta_{MPID}(s)=s^4+\frac{1}{T_D}s^3+(\omega_R^2+\frac{K_DK_S}{T_DJ_M})s^2$$
$$+\frac{J_M\omega_R^2+K_PK_S}{T_DJ_M}s+\frac{K_IK_S}{T_DJ_M} \tag{37}$$

VI. Stability Analysis

Stability is one of the most important concerns in power system operation and control. It is noted that any feedback controller can be utilized to improve the dynamic performance and/or to increase the stability margin of the closed-loop system. Relative stability and transient performance of a closed-loop control system are directly related to the closed-loop pole-zero configurations in the s-plane. By analyzing the root of Hurwitz equation, a sufficient condition of system stability with PID control will be as follows:

$$\mathrm{K_D}>\frac{\mathrm{J_MK_I}}{\mathrm{K_PK_S}+\mathrm{J_M}\omega_\mathrm{R}^2} \tag{38}$$

$$\mathrm{K_I}<\frac{\mathrm{K_D}(\mathrm{K_PK_S}+\mathrm{J_M}\omega_\mathrm{R}^2)}{\mathrm{J_M}} \tag{39}$$

Figs. 13 and 14 present the root locus of the close-loop system to the variation of the derivative gain and integral gain respectively.

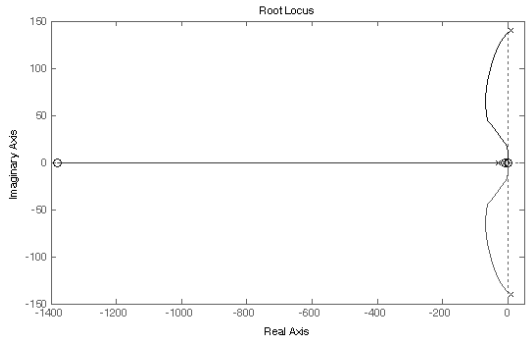

Fig. 13: Root locus diagram of close-loop system to variation of derivative gain

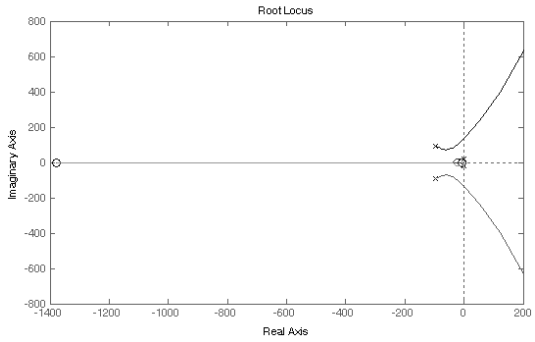

Fig. 14: Root locus diagram of close-loop system to variation of integral gain

The Nyquist diagram for two different derivative gains, stable and non-stable close-loop system have been shown in Figs. 15.

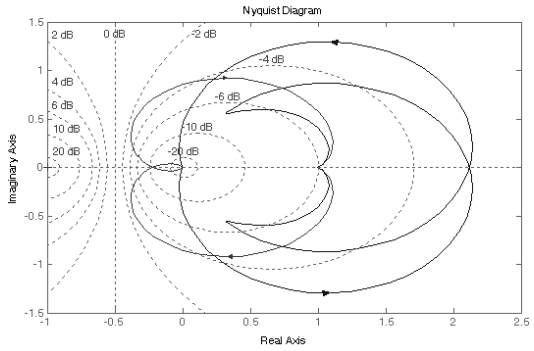

Fig. 15: Nyquist diagram for two different derivative gains

VII. Simulation Results

Performances of dynamic systems are usually defined with their transient responses. This depends highly on the performance criteria of the design such as the rise time, overshoot, settling time, largest magnitude of the actuating signal. Here simulation results obtained using Matlab are given, in which effects of parameters on the steady-state and dynamic performance of the two-mass system with controller is proposed. Various transfer functions describing a step response of the motor speed following step torque and load disturbance torque are derived. Parameters of PID controller for change in ω_G have been shown in Table III with ITAE criterion, Table IV with PPC criterion and Table V with CDM criterion. Step responses of all gains controller are plotted in the same figure in order to compare different cases (Figs. 16, 17 and 18). It is clear that the damping increases, and there is no oscillation in the system response. However, there is still a large overshoot and steady-state error in the shaft torque and response is even worse.

TABLE III
GAINS CONTROLLER WITH ITAE CRITERION

frequency ratio	A	b	c
$\frac{\omega_G}{\omega_R}$	1	$\frac{3}{\sqrt{5}}$	$\sqrt{3.3}$
K_P	0	2.6326	7.5686
K_I	287.1694	457.6968	905.3070
K_D	0.0571	0.0676	0.0837

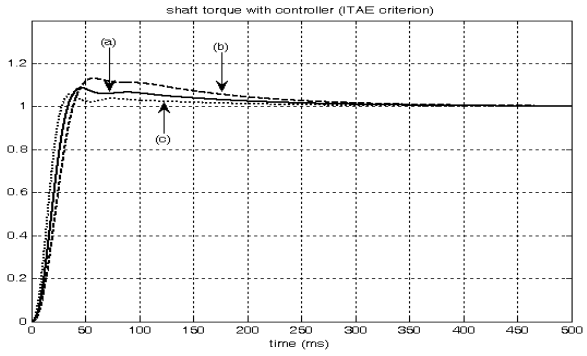

Fig. 16: Shaft torque with PID controller with ITAE criterion

TABLE IV
GAINS CONTROLLER WITH PPC CRITERION

frequency ratio	A	b	c
$\frac{\omega_G}{\omega_R}$	1	$\frac{3}{\sqrt{5}}$	$\sqrt{3.3}$
K_P	0	3.6326	9.3046
K_I	74.6854	271.2989	639.9494
K_D	0.0118	0.0430	0.1015

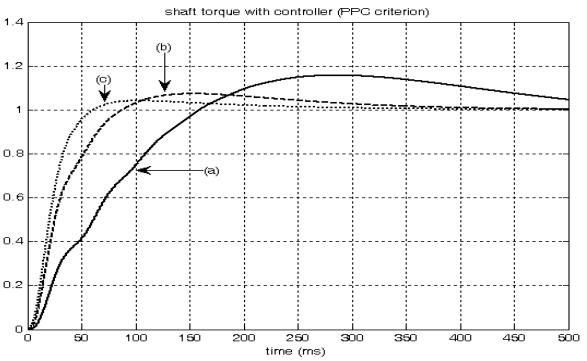

Fig. 17: Shaft torque with PID controller with PPC criterion

TABLE V
GAINS CONTROLLER WITH ITAE CRITERION

frequency ratio	a	b	c
$\frac{\omega_G}{\omega_R}$	1	$\frac{3}{\sqrt{5}}$	$\sqrt{3.3}$
K_P	0	2.6326	7.5686
K_I	256.0595	424.1632	807.2324
K_D	0.0677	0.0801	0.0992

TABLE VI
GAINS CONTROLLER WITH ITAE CRITERION

coefficients	CDM	ITAE	PPC	PPC +ITAE
K_P	0	0	1.0859	5.1617
K_I	256.0595	287.1694	74.6854	355.0132
K_D	0.0677	0.0571	0.0118	0.0563

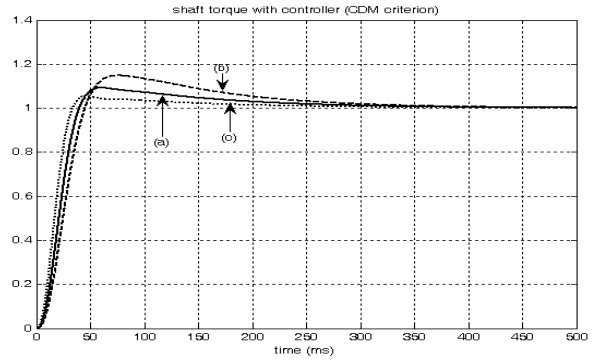

Fig. 18: Shaft torque with PID controller with CDM criterion

PID controller gains for different criteria are summarized in Table VI. Fig. 19 show the step response of shaft torque for different criteria. The shaft torque with PID controller and compensation has been shown in Fig. 20. It is clear that with CDM+ITAE criterion the performance response is better. Fig. 21 and Fig. 33 show the step response of the shaft torque and response frequency of close-loop system for PID and MPID controller respectively.

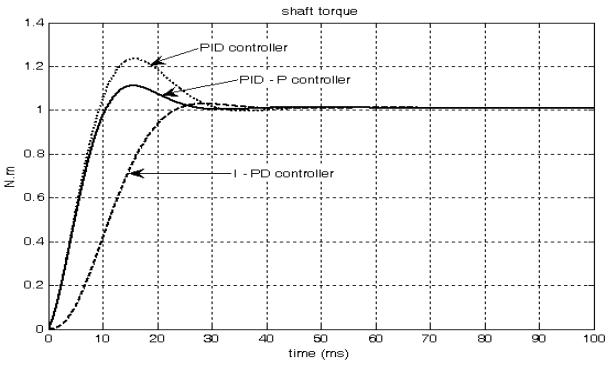

Fig. 19: Shaft torque with PID controller and different criterion

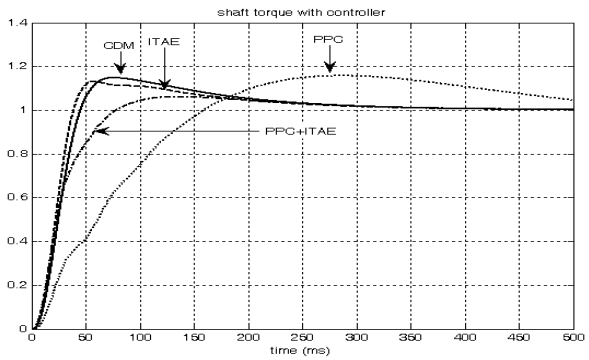

Fig. 20: Shaft torque with PID controller and compensation

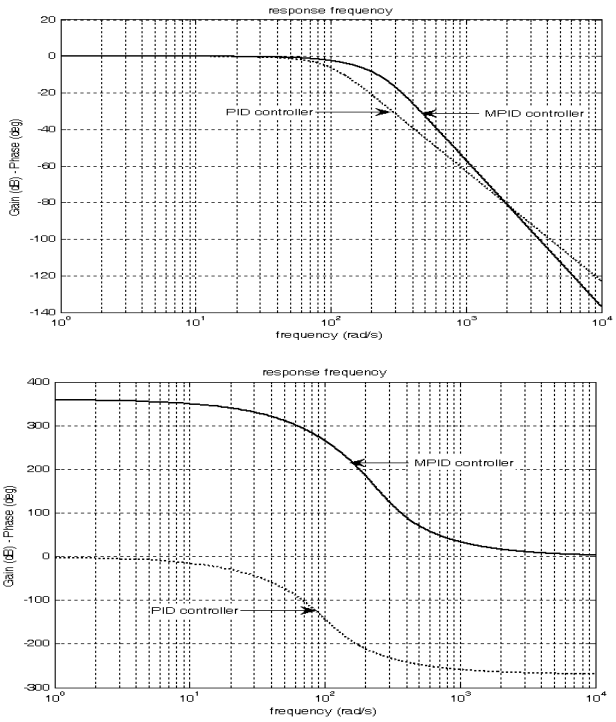

Fig. 21: Response frequency of close-loop system with PID and MPID controller

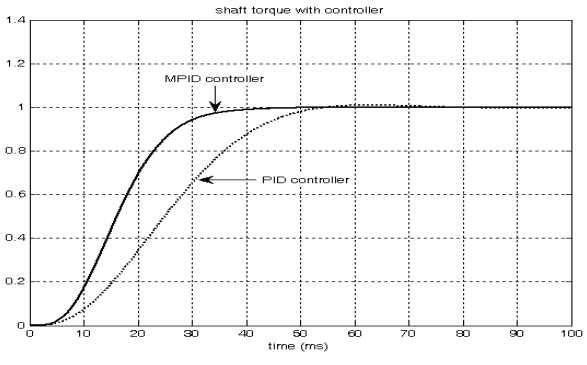

Fig. 22: Shaft torque with PID controller and MPID controller

VIII. Conclusion

Modeling and systematic dynamic analysis of a two mass resonant system have been presented by deriving a small signal plant and torque control model. Response of the system was studied for torque command and load disturbance torque. Control system design for the shaft torque of a two-mass system was realized by CDM which is an algebraic method involving only polynomials. The analysis was validated by a time domain simulation and controlled system was tested to be successful by Matlab/Simulink program.

Acknowledgements

This work has been extracted from the research project entitled “Dynamic eigenvalue analysis and simulation of two-mass resonant system with PID controller” in Islamic Azad University – Najaf Abad Branch, Esfahan, Iran.

References

[1] J.Wang, Y.Zhang, L.Xu, Y.Jing, S.Zhang, “Torsional vibration suppression of rolling mill with constrained model predictive control”, IEEE/VVICA, Vol.2, pp.6401-6405, June 2006.

[2] K.Erenturk, “Nonlinear two-mass system control with sliding-mode and optimized proportional-integral derivative contoroller combined with a grey estimator”, IET Contr. The. Apll., Vol.2, No.7, pp.635-642, 2008.

[3] S.Katsura, K.Ohnishi, “Force servoing by flexible manipulator based on resonance ratio control”, IEEE Trans. On Indu. Elec., Vol.54, No.1, pp.539-547, February 2007.

[4] J.S.Kim, L.W.Yang, Y.S.Kim, Y.J.Kim, “The vibration suppression control of the two mass resonant system using the H_∞ filter”, IEEE/IECON, Vol.3, pp.1464-1470, Aug./Sep. 1998.

[5] B.Nam, H.Kim, H.Lee, D.Kim, “Optimal speed controller design of the two-inertia stabilization system”, PWASET Vol.31, pp.155-160, July 2008.

[6] K.Szabat, T.Orlowska-Kowalska, “Optimization of the two-mass drive dynamics using different compensation feedbacks”, IEEE/OPTIM, pp.19-24, May 2008.

[7] S.Suathed, S.Nundrakwang, T.Benjanarasuth, J.Ngamwiwit, N.Komine, “Simplified design of I-P controller for speed of two-inertia system”, IEEE Tran. on Cont. Sys., Vol.27, No.1, pp.1900-1904, January 2008.

[8] K.Peter, I.Scholing, B.Orlik, “Robust output feedback H_∞ control with a nonlinear observer for a two-mass system”, IEEE Trans. Ind. Appl., Vol.6, No.2, pp.637-644, 2003.

[9] H.Kataoka, K.Ohishi, T.Miyazaki, S.Katsura, H.Takuma, “Motion control strategy of industrial robot for vibration suppression and little positioning phase error”, IEEE/AMC, pp. 661-666,March 2008.

[10] P.Koroundi, H.Hashimoto, V.Utkin, “Discrete sliding mode control of two mass system”, IEEE/ISIE, Vol.1, pp.338-343, July 1995.

[11] T.M.O’Sullivan, C.M.Bingham, N.Schofield, “High performance control of dual-inertia servo drive systems using low cost integrated SAW torque transducers”, IEEE Tran. on Indu. Elec., Vol.55, No.4, pp.1226-1237, August 2006.

[12] K.Sugiura and Y. Hori, “Vibration suppression in 2- and 3-mass system based on the feedback of imperfect derivative of the estimated torsional torque,” IEEE Trans. Ind. Electronics, vol. IE-43, No.1, pp.56-64, Jan./Feb. 1996.

[13] S.Hashimoto, K.Hara, H.Funato, K.Kamiyama, “AR-based identification and control approach in vibration suppression”, IEEE Tran. On Ind. Appl., Vol.37, No.3, pp.806-811, May/June 2001.

[14] M.C.M.Teixeira, E.Assuncao, M.Covacic, “Proportional controllers: direct method for stability analysis and MATLAB implementation”, IEEE Tran. On Educ., Vol.50, No.1, pp.74-78, Feb. 2007.

[15] T.M.O’Sullivan, C.M.Bingham, N.Schofield, “Enhanced servo control performance of dual-mass systems”, IEEE Tran. on Indu. Elec., Vol.54, No.3, pp.1387-1398, June 2007.

[16] Y.Wu, K.Fujikawa, H.Kobayashi, "A torque control method of two mass resonant system with PID-P controller", IEEE/AMC, pp.240-245, 1998.

Authors’ information

[1]Department of Electrical Engineering, Islamic Azad University, Najaf Abad Branch, Najaf Abad, Esfahan, Iran.

[2]School of Electrical and Computer Engineering, Faculty of Engineering, University of Tehran, Iran.

Ghazanfar Shahgholian was born in Esfahan, Iran, on December 7, 1968. He graduated in electrical engineering from Esfahan University of Technology (IUT), Esfahan, Iran, in 1992. He received the M.Sc and PhD in electrical engineering from University Tabriz, Tabriz, Iran in 1994 and from Islamic Azad University, Science and Research Branch, Tehran, Iran, in 2006, respectively. He is now an associate professor at Department of Electrical Engineering, Faculty of Engineering, Islamic Azad University – Najaf Abad Branch. His teaching and research interests include application of control theory to power system dynamics, power electronics and power system simulation.

Jawad Faiz received his Ph.D. in Electrical Engineering from the University of Newcastle upon Tyne, England in 1988. He is now a Professor at School of Electrical and Computer Engineering, Faculty of Engineering, University of Tehran. He is the author of 215 publications in international journals and conference proceedings. Dr Faiz is a senior member of IEEE. He is also a member of Iran Academy of Sciences. His teaching and research interests are switched reluctance and VR motors design, design and modeling of electrical machines, drives, and transformers.